

Zero-Temperature Critical Phenomena in Two-Dimensional Spin Glasses

Naoki KAWASHIMA* and Takayuki AOKI^{1,**}

Department of Physics, Tokyo Metropolitan University, Minamioshima 1-1, Hachiohji, Tokyo 192-0397, Japan

¹ *2nd System Engineering Department, NEC Microcomputer Technology, Ltd., Tsukagoshi 3-484, Saiwai, Kawasaki, Kanagawa 210-8511, Japan*

(Received October 21, 2018)

Recent developments in study of two-dimensional spin glass models are reviewed in light of fractal nature of droplets at zero-temperature. Also presented are some new results including a new estimate of the stiffness exponent using a boundary condition different from conventional ones.

KEYWORDS: critical phenomena, spin glass, disordered system, droplet picture

§1. Introduction

One of most important unresolved issues concerning disordered spin systems is whether the low-temperature phase of spin glass systems is described by the mean-field picture¹⁾ or rather by the droplet picture.²⁾ For three dimensions, the issue has not yet been settled in spite of a lot of arguments and numerical works.³⁾ On the other hand, most researchers believe that the spin glass model in two dimensions with a continuous bond distribution is disordered (paramagnetic) at any finite temperature and is critical right at the zero temperature. In this case, the critical phenomena near the zero temperature have been understood mainly by the droplet picture⁴⁾ and other similar arguments such as the domain wall renormalization group argument.⁵⁾ The droplet picture⁴⁾ can also explain fairly well the experimental results on the two-dimensional spin glass systems.⁶⁾ According to the standard droplet picture, the characteristic length scale at each temperature, i.e., the correlation length, is directly comparable to the typical size of an activated droplet. Then, it is natural to expect that the various length scales associated with the same energy (temperature) scale should be essentially the same except for some constant prefactor regardless of difference in the definitions. For example, the correlation length at temperature T should be the same as the typical droplet size whose excitation energy is $k_B T$. This yields the scaling relation

$$-\theta_D = y_t$$

where $y_t \equiv 1/\nu$ is the thermal scaling exponent, and θ_D is the droplet exponent that characterizes the size dependence of the droplet excitation energy. Another example is the stiffness exponent θ_S that relates the size of the whole system to the excitation energy of the domain wall which is induced by some appropriately chosen boundary condition. The excitation energy is called domain wall

energy or “stiffness” and hence the name of the exponent. One, then, might expect that y_t , $-\theta_D$ and $-\theta_S$ are equal to each other. In fact, in the domain wall renormalization argument,^{5,7)} it was concluded that $y_t = -\theta_S$. However, we see in what follows that a number of numerical calculations, such as the direct calculation of the magnetization as a function of magnetic field⁸⁾ and the recent direct measurement of droplet excitation energies,⁹⁾ indicate that θ_S is truly different from the other two, whereas the estimates of y_t and θ_D are at least close to each other.

In this paper, we concentrate our attention on the Edwards-Anderson (EA) models described by the following Hamiltonian,

$$\mathcal{H} = - \sum_{\langle ij \rangle} J_{ij} S_i S_j,$$

where J_{ij} is a quenched random variable with some given bond distribution. It is a general belief that models described by this Hamiltonian can be classified into two classes according to the type of the distribution of J_{ij} . One is the class of continuous distributions. The Gaussian bond distribution is the most often studied example in this category. Models in this category do not have non-trivial degeneracy in the ground states. The other class is that of discontinuous distributions to which the $\pm J$ model belongs. Models in this category in general have non-trivial degeneracy and the entropy per spin approaches to a finite value in the zero-temperature limit. In other words, the model is not completely “frozen” even at zero-temperature, making the two-point correlation function decaying to zero. As a result, they are characterized by non-zero values of the exponent η .

In section 2, we consider the model with continuous bond distribution. We review some of previous numerical calculations for models in this category focusing on the three exponents, θ_S , y_t and θ_D . We also present some new results on θ_S . In section 3, we review briefly recent results on the discontinuous distributions.

§2. Models with Continuous Bond Distributions

* E-mail: nao@phys.metro-u.ac.jp

** E-mail: t-aoki@nmit.tmg.nec.co.jp

2.1 Domain-wall renormalization-group argument and stiffness exponent

It was argued⁵⁾ that the excitation energy $E_W(L)$ of a

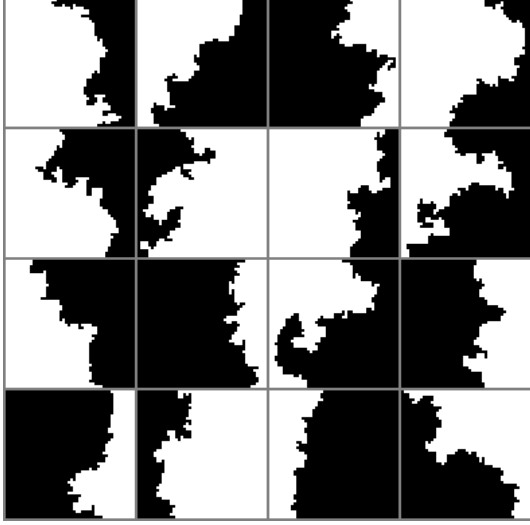


Fig. 1. The domain walls in 16 randomly chosen samples with $L = 48$.

domain wall across a system of size L can be regarded as the renormalized coupling constant after the system is renormalized up to scale L . It follows that if we define the scaling exponent θ_S by

$$E_W(L) \propto L^{\theta_S},$$

θ_S is expected to equal y_t . Also, in the standard droplet theory for spin glasses,²⁾ $E_W(L)$ is considered to be of the same order as the excitation energy of a droplet of scale L . If these interpretations are correct, we can estimate the thermal exponent y_t or the droplet exponent θ_D simply by measuring the domain wall energy for systems of various sizes instead of computing derivatives of the free energy or the droplet excitation energy. In fact, it is technically much easier to compute the domain wall energies than droplet excitation energies. This is one of the reasons why in the early stage of the study on spin glasses in two dimensions, many works were devoted to computation of the domain wall energy. We can see this in Table I. In Table I, some of previous numerical works for estimating one or two of the three scaling exponents, y_t , θ_S and θ_D , for models with continuous, mostly Gaussian, bond distributions in two dimensions are listed in chronological order.

The first estimate of the stiffness exponent was carried out through the numerical transfer matrix method by McMillan.⁷⁾ He applied the periodic or anti-periodic boundary condition in one direction while replicating the same $L \times L$ system periodically in the other direction to obtain a long strip, thereby mimicing the periodic boundary condition. The width of the widest strip was $L = 8$. By switching from the periodic boundary condition to the anti-periodic one, a domain wall is created across the strip. The excitation energy of such domain walls

at zero-temperature was estimated through an extrapolation of the domain wall free energy at finite temperatures to zero temperature. The resulting estimate of the stiffness exponent was

$$-\theta_S = 0.281(5). \quad (2.1)$$

Bray and Moore⁵⁾ used the zero-temperature transfer matrix method in order to directly calculate the domain wall energy for slightly larger L 's than McMillan's previous calculation. Instead of using periodic or antiperiodic boundary condition for creating domain walls, they dealt with $L \times (L + 1)$ systems with periodic boundary condition in the direction of L and randomly fixed boundary condition in the direction of $L + 1$. Domain walls were created by simultaneous inversion of all the fixed spins on one of two boundaries perpendicular to the direction of $L + 1$. They obtained an estimate of the stiffness exponent only slightly smaller than Eq. (2.1).

McMillan¹³⁾ obtained another estimate of the stiffness exponent based on zero-temperature stiffness calculation through a heuristic optimization. An ordinary Monte Carlo method at a finite temperature was used for generating many initial spin configurations. By quenching these spin configurations, approximate solutions were obtained. If the number of trials is large enough, i.e., if one generates sufficiently many approximate solutions, one can expect that the solution with the lowest energy among them coincides the true ground state with fairly large probability. In this way, $L \times L$ systems with periodic boundary condition were examined up to $L = 8$. The resulting estimate turned out to be consistent with the above two estimates.

Rieger et al.¹⁷⁾ performed a similar calculations on a much larger scale with periodic boundary condition in both the directions. They dealt with systems up to $L = 30$ using an exact optimization method based on the branch-and-cut algorithm.²⁰⁾ They obtained a value in good agreement with Eq. (2.1).

Matsubara et al.¹⁹⁾ argued that the value of the stiffness exponent depends on the boundary condition. They performed a Monte Carlo simulation on systems of $L \times (L + 1)$ up to $L = 22$. For the first system, the periodic and the free boundary condition was applied to the direction of L and $L + 1$, respectively. Then, for the second system, spins on one of the two boundaries perpendicular to the direction of $L + 1$ are fixed as they are in the ground state of the first system while those on the other boundary are fixed opposite to the first system. The boundary condition in the other direction, i.e., the direction of L , remains to be periodic. They obtained an estimate of the stiffness exponent significantly larger than previous estimates. They argued that the stiffness tends to be estimated smaller when periodic boundary condition is imposed because it introduces an additional tension into a system, and this was why they used free boundary condition for the first system.

In order to check if the stiffness exponent depends on the boundary condition, we perform a numerical calculation of domain wall energy applying free boundary condition in every direction for the first system. For the

Table I. Some of previous estimates of scaling exponents for the two dimensional EA model with the continuous bond distribution. The bond distribution is Gaussian for all the works listed here except for two items with footnotes. T_{\min} is the lowest temperature at which the computation for the largest system was performed. In the last column, TM, MC, HO, EO and FF stand for the numerical transfer method (TM), the Monte Carlo simulation (MC), a heuristic optimization (HO), an exact optimization (EO) and mapping to a free fermion problem (FF), respectively

Authors	$-\theta_S$	y_t	$-\theta_D$	Size and Boundary Condition	T_{\min}	Method
Cheung & McMillan ¹²⁾	0.34(3) ^[1]			11 (periodic) \times ∞	≥ 0.15	TM
McMillan ⁷⁾	0.281(5)			8 (periodic) \times 8 (p.t. ^[2])	≥ 0.3	TM
Bray & Moore ⁵⁾	0.291(2)			13 (randomly fixed) \times 12 (periodic)	0	TM
McMillan ¹³⁾	0.306(15)			8 (periodic) \times 8 (periodic)	0	HO
Huse & Morgenstern ¹⁰⁾ [3]	0.24(3) ^[1]			8 (periodic) \times ∞	0	TM
Cieplak & Banavar ¹⁴⁾	0.31(2)			10 (randomly fixed) \times 11 (periodic)	0	TM
Kawashima & Suzuki ⁸⁾		0.476(5)		20 (periodic) \times 20 (periodic)	0	HO
Kawashima et al. ¹⁵⁾		0.48(1)		16 (periodic) \times 16 (free)	≥ 0.1	TM
Liang ¹⁶⁾		0.50(5)		128 (periodic) \times 128 (periodic)	≥ 0.4	MC
Rieger et al. ¹⁷⁾	0.281(2)			30 (periodic) \times 30 (periodic)	0	EO
Rieger et al. ¹⁷⁾		0.48(1)		60 (periodic) \times 60 (periodic)	0	EO
Nifle & Young ¹⁸⁾		0.55(7)		20 (periodic) \times 20 (periodic)	≥ 0.8	MC
Huse and Ko ¹¹⁾ [4]		0.37 ^[5]		40 (p.t.) \times 40 (p.t.)	—	FF
Matsubara et al. ¹⁹⁾	0.2			21 (free) \times 20 (periodic)	0	MC
Kawashima ⁹⁾			0.47(5)	49 (free) \times 49 (free)	0	HO
present	0.290(10)			48 (free) \times 48 (free)	0	EO

- (1) ... The estimate of $1/\nu_{\parallel}$. (See text)
(2) ... Periodic tiling. (See text)
(3) ... The exponential bond distribution as well as the Gaussian distribution was used.
(4) ... The distribution used was symmetric, consists of two continuous parts, and has a vanishing weight around $J \sim 0$.
(5) ... This may not be considered as an estimate of y_t . (See text)

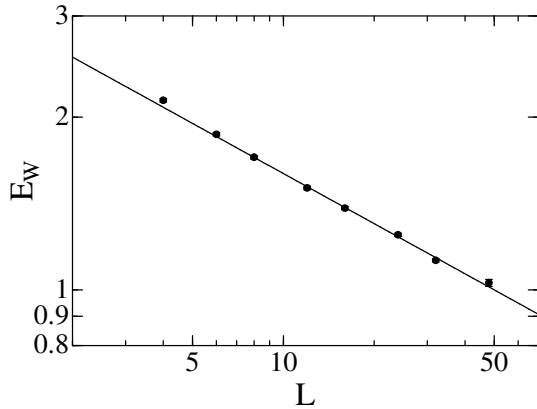


Fig. 2. The domain wall energy. The typical magnitude of statistical errors is about a quarter of the symbol size except for the error bar of $L = 48$ being slightly larger than the symbol size.

second system we apply a fixed boundary condition in one direction just as Matsubara et al. did, i.e., we fix spins on one boundary as they are in the first system and those on the other boundary opposite. We carry out our calculation for $L \times L$ systems up to to $L = 48$ using an exact optimization method.²¹⁾ In Fig. 1, some randomly chosen examples of the domain walls are illustrated.

In Fig. 2, the domain wall energy is plotted against the

system size in logarithmic scale. The linearity is rather good and the slope is estimated as

$$-\theta_S = 0.290(10)$$

in agreement with other previous results. Here, the cited error has been estimated manually after doing some trial-and-errors in the plot. This error estimate turns out relatively conservative compared to previous estimates. In fact, we should be conservative in the present case because the exponent θ_S is small in absolute value which makes the corrections to scaling relatively large. For example, if we plot the excitation energy against $L + a$ instead of L , where a is some constant term of order of unity, the estimate of θ_S would change significantly. This sort of correction due to a constant term added to the system size exists, in principle, and should be taken into account in order to make the estimate reliable. We suppose this is one of reasons for the discrepancy between our estimate and Matsubara et al.'s estimate.

We also investigate geometrical properties of domain walls. In Fig.3, averaged length along the perimeter P and the roughness R of droplets are plotted against L . Here the roughness is the difference in the x -coordinates of the left-most site and the right-most site on the domain wall. The obtained data for the perimeter can be fit well by the following scaling form

$$P \propto L^{D_W} \quad \text{where} \quad D_W = 1.28(2).$$

The estimate of D_W agrees very well with the previous estimate $D_W = 1.34(10)$ ¹⁷⁾ for systems with the peri-

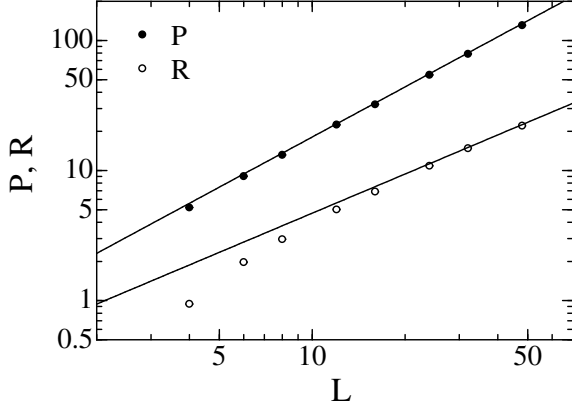


Fig. 3. The averaged perimeter P and roughness R of domain walls.

odic boundary condition. On the other hand, the data for the roughness in the logarithmic scale clearly shows a systematic decrease in the slope converging to unity around $L \sim 32$, which indicates a presence of a strong correction to scaling. However, this non-linearity can be easily accounted for by adding a constant to L as discussed above. The resulting estimate is consistent with

$$R \propto L^\zeta \quad \text{where} \quad \zeta = 1.$$

2.2 Zero-temperature finite size scaling and the thermal exponent y_t

As is discussed above, in the droplet argument or the domain-wall renormalization-group argument, we have only one characteristic length scale at each temperature. It was also concluded, based on these arguments, that all the exponents that characterize the scaling properties of various static quantities can be derived from the droplet exponent or the stiffness exponent. It should be noted, however, that we can derive this “one-parameter-scaling” without any special pictures or assumptions. Instead, we simply assume the standard finite size scaling form for the singular part of logarithm of the partition function,

$$\log Z_{\text{sing}}(T, H, L) = f(TL^{y_t}, HL^{y_h}), \quad (2.2)$$

where f is a scaling function and T, H, L are the temperature, the uniform magnetic field and the system size, respectively. From this form, we obtain for the magnetization the following expression,

$$M(T, H, L) = L^{y_h - y_t} \tilde{m}(TL^{y_t}, HL^{y_h}).$$

Since the model does not have a degeneracy in the ground state except the trivial one with respect to simultaneous inversion of all spins, the magnetization in the limit of $H \rightarrow +0$ should be proportional to $L^{d/2}$. This yields a scaling relation

$$y_h = y_t + \frac{d}{2}.$$

Therefore we have

$$M(T, H, L) = L^{d/2} \tilde{m}(TL^{y_t}, HL^{y_t+d/2}). \quad (2.3)$$

Then, it is easy to see that the zero-temperature linear susceptibility at $H = 0$ has the asymptotic form

$$\chi(T = 0, H = 0, L) \propto L^{y_t}. \quad (2.4)$$

Similarly, the magnetization at zero-temperature has the form

$$m(T = 0, H, L = \infty) \propto H^{1/\delta} \quad \text{where} \quad \delta = 1 + y_t.$$

There were some numerical attempts on computing thermodynamic quantities even before McMillan’s calculation of stiffness. Such measurements were done by Monte Carlo simulations.²²⁾ In retrospect, their estimates were affected by insufficient equilibration in the low temperature region. The first direct numerical calculation of a thermodynamic quantity after researchers started taking into account such equilibration problems was carried out through an optimization method by Kawashima and Suzuki.⁸⁾ We obtained ground states of the systems with Gaussian bond distribution, thereby measuring the magnetization at a small but finite magnetic field. In particular the zero-temperature linear susceptibility for various system sizes up to $L = 20$ was measured. By matching the resulting estimate with Eq. (2.4), the thermal exponent was estimated as

$$y_t = 0.476(5). \quad (2.5)$$

Surprisingly, the value did not agree with the stiffness exponent which had been estimated rather accurately.

From Eq.(2.2) the scaling form for the spin glass susceptibility can be also derived. Namely,

$$\begin{aligned} \chi_{\text{sg}} &\equiv \frac{1}{L^d} \sum_{ij} [\langle S_i S_j \rangle^2] \sim -\frac{1}{3L^d} \frac{\partial^4}{\partial (\beta H)^4} \log Z_{\text{sing}} \\ &\sim L^d \tilde{\chi}_{\text{sg}}(TL^{y_t}, HL^{y_t+d/2}), \end{aligned} \quad (2.6)$$

where $[\dots]$ stands for the bond configuration average whereas $\langle \dots \rangle$ the thermal average. The spin glass susceptibility was computed numerically through the transfer matrix method¹⁵⁾ for system sizes up to $L = 16$ at various temperatures. From the best fit to the form Eq.(2.6) with setting $H = 0$, the exponent y_t was estimated as

$$y_t = 0.48(1),$$

which agrees with the previous result obtained through the computation of the magnetization.

Liang¹⁶⁾ also computed χ_{SG} for larger systems by a cluster Monte Carlo method. It was at $T = 0.4$ that the simulation of the largest size ($L = 128$) was performed. The estimate of the thermal exponent was $y_t = 0.50(5)$ reconfirming the above-mentioned previous results. Assuming that the temperature dependence of the correlation length obtained by Cheung and McMillan¹²⁾ is correct down to this temperature, we can roughly estimate the correlation length at $T = 0.4$ to be a few tens of lattice constants. Therefore, Liang’s calculation can be considered complementary to the above two previous calculations, in that Liang’s calculation was performed

at temperatures higher than the cross-over temperature whereas for the two calculations mentioned above were carried out at temperatures lower than that.

The computation of the zero-temperature magnetization was also redone for larger systems. Rieger et al.¹⁷⁾ used an exact optimization method for computing the magnetization in a magnetic field for systems with periodic boundary condition. Matching the data for systems up to $L = 50$ to Eq. (2.3), they obtained an estimate of y_t essentially identical to the previous one Eq. (2.5).

Given these results on the thermal exponent together with the above mentioned estimates of stiffness exponent, it is now rather unlikely that the discrepancy between them is only a numerical artifact. If they are truly different as the numerical estimates suggest, a simple domain-wall renormalization-group argument⁵⁾ and an over-simplified droplet picture.

2.3 Droplet argument and droplet exponent

Then, how can we elaborate the droplet picture in order to explain the discrepancy? A recent work⁹⁾ on droplets may shed light on this question though the answer has not yet been obtained. “Droplet” is a well-known and

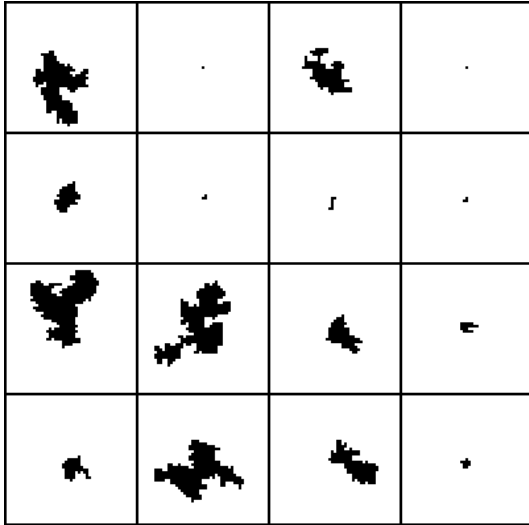


Fig. 4. Droplets of 16 randomly chosen samples.

useful concept in the study of critical phenomena.²³⁾

The droplet argument for spin glasses²⁾ based on this concept is one of important working hypotheses in the field. Droplets are collective excitations from some ordered state below the transition temperature. A naive interpretation of the droplet theory leads to the conclusion $-\theta_S = -\theta_D = y_t$. However, because of technical difficulty mentioned below, no direct observations of the droplets was carried out until quite recently. In addition, as we have seen above, at least the simplest version of the argument does not work in the present case. Therefore, the equivalence between y_t and $-\theta_D$ should be re-examined carefully.

Fisher and Huse defined²⁾ a droplet of scale λ including a given site i as a cluster of spins (with i among

them) with the smallest excitation energy that contains more than λ^d and less than $(2\lambda)^d$ spins. The basis of the argument is the following scaling form that describes the excitation-energy distribution of droplets of scale λ :

$$P_\lambda(E_\lambda) = \frac{1}{\Upsilon \lambda^{\theta_D}} \tilde{P}\left(\frac{E_\lambda}{\Upsilon \lambda^{\theta_D}}\right) \quad (2.7)$$

where Υ is some constant, θ_D is the droplet exponent, and $\tilde{P}(x)$ is the scaling function which is continuous and non-vanishing at $x = 0$. Since the droplet “size”, λ , is defined to be proportional to $(\text{volume})^{1/d}$, it is not necessarily a spanning length of droplets because the volume of a droplet may in general have a non-trivial fractal dimension. While it was argued²⁾ that the droplets must be compact if θ_D is positive, no extensive discussion had been devoted to the geometrical properties of droplets in the present two-dimensional case, where θ_D is predicted to be negative, until quite recently. We demonstrated⁹⁾ that a typical large droplet in two dimensions occupies only an infinitesimal fraction of the volume of the minimal box that can contain the droplet. It follows that for a given droplet we have at least two essentially different length scales, λ and the spanning length. We refer hereafter to the fractal dimension of the droplet volume as D . Then, we have the relation

$$V = \lambda^d \propto l^D$$

where l is the spanning length of the droplet.

Since the above-mentioned definition of droplets by Fisher and Huse is inconvenient from computational point of view, we adopted the following alternative definition. First we consider an $L \times L$ system with free boundary condition. A droplet of scale L is then defined to be the cluster of spins that has the smallest excitation energy among those which contain the central spin and contains no spins on the boundary.

If we assume the conventional droplet argument, the central spin is surrounded by droplets (in the original definition) of various scales. Considering the fact that larger droplets tend to have smaller excitation energy, one may expect that the spanning length of the droplet with the new definition would be proportional to L . We here define θ'_D by the following L dependence of the average excitation energy of the droplets in our definition,

$$[E_D(L)] \propto L^{\theta'_D}.$$

Comparing this to Fisher and Huse’s definition of the droplet, we obtain

$$\theta_D = \frac{d}{D} \theta'_D, \quad (2.8)$$

because L is proportional to the spanning length of the droplet.

In order to observe droplets with the new definition, we first computed the ground state with free boundary condition, and took it as the reference spin configuration. Then we computed the ground state with the constraint that the spins on the boundary are to be fixed as they are in the reference state while the central spin is to be fixed opposite, thereby forcing a cluster of spins including the central spin to flip. For a system with the free

boundary condition, polynomial-time optimization algorithms are available whereas for the systems with constraints no such algorithm is known. In fact, the two dimensional spin glass problem with general constraints has been proven to be NP hard.²¹⁾ Therefore, we have employed the replica optimization,⁸⁾ which is a heuristic optimization algorithm based on the idea of renormalization group. The details of the algorithm are described elsewhere.^{8, 24)}

Observed droplets varies in size and shape. Some of them contains only one spin while spanning length of some others turned out to be comparable to the system size itself (See Fig. 4). This reflects the fact that $|\theta_D|$ is small and the excitation energy does not very strongly depend on the droplet size, yielding a non-negligible probability for a small droplets being chosen. In the larger droplets, on the other hand, many handles and overhangs can be observed, which already suggests the fractal nature of the droplets. The averaged spanning length was found to be proportional to the system size as we expected.

The averaged length, P , of the boundary of the droplet and the averaged volume, V were also measured. For P , we obtained $P \propto L^{D_s}$ with the surface fractal dimension

$$D_s = 1.10(2).$$

For V , we estimated the fractal dimension as

$$D = 1.80(2). \quad (2.9)$$

The fractal dimension D of droplets is certainly smaller than $d = 2$. Thus, we concluded that the droplets at the critical point $T = 0$ have fractal nature in the volume as well as in the perimeter.

It was also found that the droplet excitation energy $E_D(L)$ have a broad distribution, similar to the size and the shape. When rescaled with the average value $[E_D(L)]$, histograms of excitation energies for various system sizes fit on top of each other, showing the validity of the scaling form Eq. (2.7). In addition, we observe that the scaling function $\tilde{P}(X)$ has a non-vanishing value at $X = 0$, satisfying a necessary condition for the droplet argument to be valid.

When $\log E_D$ is plotted against $\log L$ the slope is estimated to be -0.42 . From this value, together with two others obtained by using other measures of the droplet size instead of L , we obtained the estimate of the droplet exponent θ'_D :

$$-\theta'_D = 0.42(4). \quad (2.10)$$

Assuming Eq. (2.8) and using the value of D in Eq. (2.9), we obtained the following estimate of θ_D ,

$$-\theta_D = 0.47(5) \quad (2.11)$$

in good agreement with previous estimates of y_t such as Eq. (2.5).

2.4 Other related estimates of scaling exponents

As far as we know, the first important attempt to estimate y_t was made through the computation of correlation length.¹²⁾ The numerical transfer matrix method

was employed for strips of $L \times N$ where $L \leq 11$ and N is so large that we can take it as infinite effectively. The periodic boundary condition was imposed across the strip. Correlation lengths $\xi_{\parallel}(T, L)$ in the longitudinal direction, i.e., the direction of N , were measured at various temperatures down to $T = 0.15$. They estimated the correlation length exponent as $\nu_{\parallel} = 2.96(22)$. We should note here that this ν_{\parallel} is not necessarily equal to $\nu \equiv 1/y_t$ because of the very large aspect ratio of the systems. As we have seen above, a number of numerical results suggest that domain walls and droplets of the same length scale correspond to different energy scales, and it is the droplet excitation energy, not the domain wall energy, that scales with the thermal exponent y_t . On the other hand, in a long strip, it is the domain wall type excitations that determines the correlation between two points separated by a very long distance in the longitudinal direction. Therefore it is not very surprising that their estimate turned out to be close to θ_S , not y_t .

Another computation based on the measurement of correlation lengths was performed by Huse and Morgenstern¹⁰⁾ for models with the exponential bond distribution as well as those with the Gaussian distribution. Again, the transfer matrix method was used. The maximum width of the strip was $L = 8$. Assuming the phenomenological renormalization group relations,

$$\frac{1}{2}\xi_{\parallel}(T, 2L) = \xi_{\parallel}(T', L)$$

with

$$\frac{T'}{T} \approx 2^{-1/\nu_{\parallel}},$$

they obtained the estimate $\nu_{\parallel} \sim 4.2(5)$.

Huse and Ko¹¹⁾ carried out a unique estimation of an exponent. They considered a system that consists of an infinite periodic repetition of many $L \times L$ systems identical to each other. Since the system size is infinite, it has a phase transition, presumably, of the Ising type. Mapping the problem into a free fermion problem the eigen values of its row-to-row transfer matrix were obtained within a polynomial computational resources. Transition temperatures, then, correspond to those at which the gap between the largest and the second largest eigen values vanishes. Assuming that the typical transition temperature is proportional to L^{-y_t} where L is the size of the unit cell, they obtained an estimate $y_t = 0.37$. However, again because of the existence of multiple length scales, it is not clear whether the exponent estimated in this way should be considered as y_t .

§3. Discontinuous Bond Distributions

The critical behavior of the systems with discontinuous bond distributions is believed to be qualitatively different from the continuous distribution discussed in the last section because of the high degeneracy in the ground state. In this case the critical properties are not as fully understood as in the case of continuous distributions. What is missing is a theory corresponding to the droplet argument for the case of continuous distributions.

The bond distribution in this class that is most often

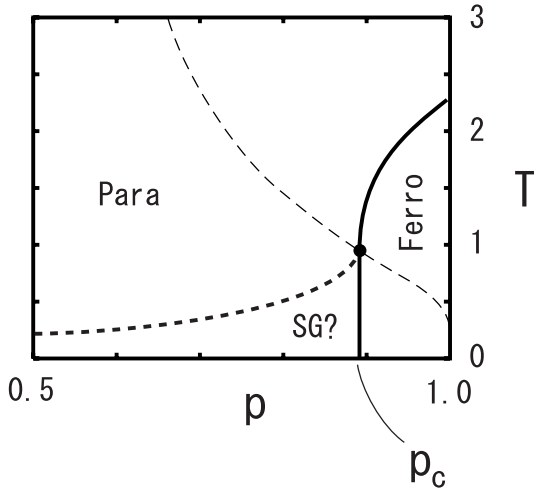


Fig. 5. The schematic phase diagram of $\pm J$ model on a square lattice. The thin dashed line stands of the Nishimori line, not a phase boundary, whereas the dotted line stands for a speculative phase boundary which has not yet been confirmed.

considered is the binary bond distribution where a coupling J_{ij} takes on the value $+J$ and $-J$ with probability p and $1-p$, respectively. For this bond distribution, the possibility of a finite temperature phase transition even in the case of the symmetric distribution ($p = 1/2$) has not been ruled out^{25,26} as mentioned below.

3.1 Intermediate Phase?

Another problem that had been remaining to be solved until recently concerns the $p-T$ phase diagram of the models with asymmetric binary bond distributions. It had been suggested^{27,28,29} that some intermediate phase exists in the $p-T$ phase diagram close to the vertical part of the phase boundary (See Fig. 5) between the ferromagnetic phase and the other, presumably paramagnetic, phase. The suggestion was made based on zero-temperature numerical calculations. For the site-random model the evidence for the existence of an intermediate phase seemed to be even stronger than for the bond-random model.^{30,31}

We reinvestigated³⁷ this issue by studying the domain wall energy at zero temperature via the determination of exact ground states for large system sizes ($L \leq 32$) and large number of samples ($N_{\text{sample}} \geq 32768$) using a polynomial algorithm described by Barahona et al.²⁷ We calculated the domain wall energy E_W for various system sizes with various ferromagnetic bond concentration p , applying the periodic or the anti-periodic boundary condition in one direction and the free boundary condition in the other. The stiffness exponent θ_S and another exponent ρ defined by

$$[E_W] \propto L^\rho \quad (3.1)$$

were estimated. A positive value for ρ signifies the stability of a ferromagnetic ground state even in the presence of thermal fluctuations and therefore the existence of the

ferromagnetic long range order at finite temperature.⁵⁾ We defined $p_c^{(1)}$ and $p_c^{(2)}$ as the critical concentrations of ferromagnetic bonds at which $[E_W]$ and $[E_W^2]^{1/2}$, respectively, change from increasing to decreasing as functions of L .

We hypothesized the following finite size scaling forms for E_W and E_W^2

$$[E_W]L^{\psi^{(1)}} = f_1((p - p_c^{(1)})L^{y_p^{(1)}}), \quad (3.2)$$

$$[E_W^2]^{1/2}L^{\psi^{(2)}} = f_2((p - p_c^{(2)})L^{y_p^{(2)}}). \quad (3.3)$$

The parameters were estimated as follows.

$$p_c^{(1)} = 0.896(1), \quad y_p^{(1)} = 0.77(1), \quad \psi^{(1)} = -0.19(2) \quad (3.4)$$

$$p_c^{(2)} = 0.894(2), \quad y_p^{(2)} = 0.79(6), \quad \psi^{(2)} = -0.16(4) \quad (3.5)$$

The value of $p_c^{(1)}$ is consistent with most of previous estimates such as 0.88(2),³⁸ 0.89(2)²⁷ and 0.89(1)³⁹ while inconsistent with 0.885(1).²⁹ The estimate of $p_c^{(2)}$ is larger than but marginally consistent with all the previous estimates such as 0.86(2),⁴⁰ 0.85²⁷ and 0.870,⁴¹ while it is clearly inconsistent with 0.854(2).²⁹ The coincidence between $p_c^{(1)}$ and $p_c^{(2)}$ suggests the absence of the intermediate phase.

It is also remarkable that not only $p_c^{(2)}$ but also $y_p^{(2)}$ and $\psi^{(2)}$ agree with the corresponding values in Eq. (3.4) within the statistical errors. While the agreement in p_c already suggests the absence of the intermediate phase, we consider the agreement in the critical indices as another evidence for the absence of the intermediate spin-glass phase, since otherwise it is hardly imaginable that the first and the second moment of E_W show the same critical behavior at different values of p_c .

We also computed the stiffness for the site-random model. We found that $p_c^{(1)}$ and $p_c^{(2)}$ for the site-random model agreed with each other and that the first and the second moments were scaled with the same scaling exponents as the bond-random model mentioned above, though with larger corrections to scaling.

Prior to our work, Nishimori argued⁴³ that the phase transition is of purely geometrical nature, which leads to the strictly vertical phase boundary that separates the ferromagnetic phase from the paramagnetic (or glassy) phase in the low temperature region. If this is the case, the value of p_c at $T = 0$ must coincide that of the multicritical point, i.e., the solid circle in the phase diagram Fig. 5. The most recent calculation for the multicritical point was done by Ozeki and Ito,⁴⁵ who performed Monte Carlo simulations at finite temperatures along the Nishimori line to locate precisely the multicritical point in the phase diagram. It is unsettling that previous estimates of $p_{\text{m.c.}}$,^{44,42} including Ozeki and Ito's estimate $p_{\text{m.c.}} = 0.8872(8)$, are slightly smaller than our estimate of p_c beyond the extent of errors although the difference is rather small. The easiest explanation is that systematic errors might not be fully taken into account in the estimates, resulting in an underestimate of the errors. Another possibility is that the size dependence, Eq. (3.2) and Eq. (3.3), assumed in the estimation of the exponents may not correctly describe the true behavior. The

last possibility is that the phase boundary may not be strictly vertical in spite of Nishimori's argument. So far, we have not yet identified the reason for the discrepancy.

3.2 Relation to the Percolation Transition

We should notice the coincidence between the exponent $y_p^{(1)}$ (or $y_p^{(2)}$) in the above mentioned work³⁷⁾ with the scaling exponent $y_p \equiv 1/\nu_p$ where ν_p is the correlation length exponent for the percolation transition in two dimensions. Related to this finding, in a work preceding our estimation of $y_p^{(1)}$ and $y_p^{(2)}$, Singh and Adler⁴²⁾ investigated the critical behavior around the multicritical point, and discussed its relation to the percolation transition. They suggested that one of the two scaling axes at the multicritical point is parallel to the Nishimori line whereas the other is parallel to the temperature axis. They estimated the scaling exponent which corresponds to our $y_p^{(1)}$ and found that the value agrees with the percolation exponent. Since, according to Nishimori's argument, the temperature plays no essential role along the vertical part of the phase boundary, we could argue that the phase transitions across the boundary are characterized by the same scaling exponent independent of the temperature, although we are not sure if the argument should be valid at the two end points as well.

3.3 Finite-Temperature Phase Transition at $p = 1/2$?

In the case of the bond-random $\pm J$ model with $p = 1/2$, the majority of researchers tend to think that there is no phase transition at a finite temperature. This general belief is based on results of Monte Carlo simulations,^{32,33)} high-temperature series expansion,³⁴⁾ and the estimates of the domain wall energy.^{5,14,29)} The data from Monte Carlo simulations are not available at very low temperature, e.g., below $T = 0.4$ in Bhatt and Young's simulation,³²⁾ which makes it difficult to exclude the possibility of the transition at a temperature smaller than 0.4. Although the results of high-temperature series expansion also suggested the absence of the finite temperature phase transition, it was not very conclusive. As for the calculations of the domain wall energy, the "stiffness" exponent turned out to be even smaller in absolute value than that for the continuous distributions. Therefore, it was not very clear if θ_S is really negative. For example, the data in Cieplak and Banavar's paper¹⁴⁾ clearly shows a systematic positive curvature in the plot of the domain wall energy versus the system size. In short, so far we have not obtained very convincing evidences supporting the general belief, i.e., the absence of the phase transition at a finite temperature in two dimensions.

On the other hand, results of Monte Carlo simulation at lower temperatures were reported³⁵⁾ indicating a transition at $T \simeq 0.24$ for the $\pm J$ model with $p = 1/2$. A finite temperature phase transition was suggested³⁶⁾ also for the model with another discrete distribution where a bond variable takes on J or $-aJ$ where $0 < a < 1$. In addition, $\theta_S = 0$ was suggested²⁹⁾ based on estimates of the domain-wall energy. These results are consistent with a finite temperature phase transition for which the low-temperature phase is only marginally or weakly or-

dered, i.e., the two-point spin-spin correlation function decreases algebraically as a function of the distance.

On this issue, we found³⁷⁾ that the stiffness decreases systematically but it does so extremely slowly in the case of $p = 1/2$. The obtained data was consistent with the algebraic decrease as a function of the system size with the stiffness exponent $\theta_S = -0.056(6)$. However, we should note that the quoted error here only includes the estimated statistical error that is obtained in the standard procedure of the method of least squares. Because of the very weak dependency on the system size, the systematic error is more important here than the statistical error. Since the systematic error is difficult to estimate, other scenarios, such as convergence to a finite constant²⁹⁾ or logarithmic decay, are equally probable. If either one of these scenarios is correct, we cannot determine based solely on calculations of the stiffness exponent whether the long-range order persists at a low but finite temperature. At the moment, what we can conclude is only that the low-temperature phase is only weakly ordered even if the phase transition takes place at a finite temperature.

Very recently, Kitatani and Sinada²⁶⁾ performed an interesting numerical calculation of spin glass susceptibility and its Binder ratio. Based on the invariant properties under the gauge transformation, they constructed a new method for computing cumulants of Edwards-Anderson order-parameter at any temperature using a novel Monte Carlo method in the bond configuration space rather than in the spin configuration space. Their results of the finite size scaling analysis, appeared to suggest the existence of a phase transition around $T = 0.3$. However, based on the data analysis with corrections to scaling, they concluded that the scenario of the zero-temperature phase transition could explain their data as well.

§4. Concluding Remarks

We have reviewed recent developments in study of spin glass models in two dimensions. It has become clear in the case of continuous bond distributions that the critical behavior is dominated by fractal droplets in contrast to the compact droplets in conventional droplet argument for higher dimensions.

The disagreement between the droplet exponent and the stiffness exponent remains unsettling. At least, however, the present result suggests that a domain wall of a $L \times L$ system may not necessarily be considered as an object of scale L because of the existence of different ways for measuring the size of the same object. In other words, at present we do not know which way of measuring we should use for comparing the size of a domain wall with that of a droplet.

The models with discrete distributions are relatively poorly understood. It is an important and challenging future problem to determine whether a finite temperature phase transition takes place or not by larger scale numerical calculations.

Although it is not yet clear whether fractal objects similar to the present two-dimensional case can be defined at the critical point in higher dimensions, it is certainly worth thinking about such a possibility. The es-

sential difference would be that η is not in general zero in higher dimensions whereas $\eta = 0$ for continuous distributions making the theory simpler in the latter case. Provided that the $\pm J$ model in two dimensions is critical at $T = 0$, the same remark may apply to this discrete model since η is non-vanishing there, too. Therefore, we may obtain some new perspective for both the finite-temperature transition in three dimensions and the zero-temperature critical behavior for discrete distributions in two dimensions by generalizing the concept of zero-temperature fractal droplets to the cases with non-vanishing η .

Acknowledgements

This work is supported by Grant-in-Aid for Scientific Research Program (No.11740232) from Mombusho, Japan.

-
- [1] G. Parisi: Phys. Lett. **73A** (1979) 203; G. Parisi: J. Phys. A **13** (1980) L115, 1101 and 1887.
 - [2] D. S. Fisher and D. A. Huse: Phys. Rev. Lett. **56** (1986) 1601; D. S. Fisher and D. A. Huse: Phys. Rev. B **38** (1987) 373; D. S. Fisher and D. A. Huse: Phys. Rev. B **38** (1987) 386.
 - [3] For example see, E. Marinari, G. Parisi and J. J. Ruiz-Lorenzo: unpublished (cond-mat 9904321), and references therein; T. Komori, H. Yoshino and H. Takayama: to appear in J. Phys. Soc. Jpn. (cond-mat 9904143).
 - [4] D. S. Fisher and D. A. Huse: Phys. Rev. B **36** (1987) 8937.
 - [5] A. J. Bray and M. A. Moore: J. Phys. C **17** (1984) L463.
 - [6] G. G. Kenning, J. Slaughter and J. A. Cowen: Bull. Am. Phys. Soc. **32** (1987) 630.
 - [7] W. L. McMillan: Phys. Rev. B **29** (1984) 4026.
 - [8] N. Kawashima and M. Suzuki: J. Phys. A: Math. Gen. **25** (1992) 1055.
 - [9] N. Kawashima: unpublished (cond-mat 9910366).
 - [10] D. A. Huse and I. Morgenstern: Phys. Rev. B **32** (1985) 3032.
 - [11] D. A. Huse and L.-F. Ko: Phys. Rev. B **56** (1997) 14597.
 - [12] H.-F. Cheung and W. L. McMillan: J. Phys. C **16** (1983) 7033.
 - [13] W. L. McMillan: Phys. Rev. B **30** (1984) 476.
 - [14] M. Cieplak and J. R. Banavar: J. Phys. A **23** (1990) 4385.
 - [15] N. Kawashima, H. Hatano and M. Suzuki: J. Phys. A: Math. Gen. **25** (1992) 4985.
 - [16] S. Liang: Phys. Rev. Lett. **69** (1992) 2145.
 - [17] H. Rieger et al: J. Phys. A **30** (1997) 3939.
 - [18] M. Ney-Nifle and A. P. Young: J. Phys. A **30** (1997).
 - [19] F. Matsubara, T. Shirakura and M. Shiomi: Phys. Rev. B **58** (1998) R11821.
 - [20] M. Grötschel, M. Jünger and G. Reinelt: in Heidelberg Colloquium on Glassy Dynamics and Optimization, ed. L. van Hemmen and I. Morgenstern (Springer-Verlag, Heidelberg 1985).
 - [21] F. Barahona, R. Maynard, R. Rammal and J. P. Uhry: J. Phys. A **15** (1982) 673.
 - [22] Kinzel and K. Binder: Phys. Rev. Lett. **50** (1983) 1509.
 - [23] M. E. Fisher: Physics **3** (1967) 255.
 - [24] N. Kawashima: unpublished.
 - [25] F. Matsubara, T. Shirakura and M. Shimoi: Phys. Rev. B **58** (1998) R11821.
 - [26] H. Kitatani and A. Sinada: unpublished (cond-mat 9908370).
 - [27] F. Barahona: J. Phys. A **15** (1982) 3241.
 - [28] R. Maynard and R. Rammal: J. Phys. Lett. (France) **43** (1982) L347.
 - [29] Y. Ozeki: J. Phys. Soc. Jpn. **59** (1990) 3531.
 - [30] T. Shirakura and F. Matsubara: J. Phys. Soc. Jpn. **64** (1995) 2338.
 - [31] Y. Ozeki and Y. Nonomura: J. Phys. Soc. Jpn. **64** (1995) 3128.
 - [32] R. N. Bhatt and A. P. Young: Phys. Rev. B **37** (1988) 5606.
 - [33] I. Morgenstern and K. Binder: Phys. Rev. Lett. **43** (1979) 1615.
 - [34] R. Singh and S. Chakravarty: Phys. Rev. B **36** (1987) 559.
 - [35] T. Shirakura and F. Matsubara: J. Phys. Soc. Jpn. **65** (1996) 3138.
 - [36] T. Shirakura and F. Matsubara: Phys. Rev. Lett. **79** (1997) 2887.
 - [37] N. Kawashima and H. Rieger: Europhys. Lett. **39** (1997) 85.
 - [38] I. Morgenstern and K. Binder: Phys. Rev. B **22** (1980) 288.
 - [39] Y. Ozeki and H. Nishimori: J. Phys. Soc. Jpn. **56** (1987) 1568 and 3265.
 - [40] A. Sadiq, R. A. Tahir-Kheli, M. Wortis and N. A. Bhatti: Phys. Lett. **84 A** (1981) 439.
 - [41] Y. Ozeki: in "Computational Physics as a New Frontier in Condensed Matter Research" edited by H. Takayama et al, (The Physical Society of Japan, 1995) p.242.
 - [42] R. Singh and J. Adler: Phys. Rev. B **54** (1996) 364.
 - [43] H. Nishimori: J. Phys. Soc. Jpn. **55** (1986) 3305.
 - [44] Y. Ozeki and H. Nishimori: J. Phys. Soc. Jpn. **56** (1987) 3265.
 - [45] Y. Ozeki and N. Ito and Y. Ozeki: J. Phys. A **31** (1998) 5451.